Properties of Multilayered Nanoscale TiN/MoN Coatings, Fabricated Using Arc Evaporation

A.D. Pogrebnjak[1,*], O.V. Bondar[1], G. Abadias[2], D. Eyidi[2], B. Zhollybekov[3]

[1] *Sumy State University, 2, Rymsky Korsakov Str., 40007 Sumy, Ukraine*
[2] *P' Institute, University of Poitiers, Poitiers, France*
[3] *Karakalpak State University, Nukus, Uzbekistan*

Using vacuum-arc evaporation method we fabricated periodic multilayered TiN/MoN coatings with different bilayer periods ranging from 8 to 100 nm. We found that MoN and TiN layers grown on steel substrate show local partial epitaxy and columnar growth across interfaces. A Mo-Ti-C interlayer was observed between the substrate and the multilayered coating. MoN and TiN layers contain small (5÷30 nm) grains and are well crystallized with (100) preferred orientation. They were identified as stoichiometric fcc TiN and cubic γ-Mo₂N. Non-cubic molybdenum nitride phases were also detected. The hardness of the obtained structures achieved great values and maximal hardness was 31÷41.8 GPa for multilayered structure with 8 nm period. Fabricated coatings are perspective for using as protective coatings in order to improve mechanical characteristics of different construction materials.

1. INTRODUCTION

Such metals as Titanium and Molybdenum are widely used in modern industry as basic elements for coatings with high functional properties, for example nitride coatings. We would like to mention, that multilayered, multicomponent and nanostructured coatings are widely used in modern materials science for increasing of protective properties of different industrial products, and for improving their hardness, wear and corrosion resistance, oxidation resistance under the influence of high temperatures and so on [1 – 10].

Ion-plasma deposition or deposition of coatings using vacuum arc cathode evaporation is a very promising way of fabrication of protective coatings [1 – 8]. So we investigated TiN/MoN multilayered coatings with different bilayer periods from 8 to 100 nm. Improving the properties of such coatings using multicomponent or multilayered systems seems to be a very actual task nowadays.

2. EXPERIMENTAL DETAILS

TiN/MoN samples were deposited on A 570 Grade 36 and AISI M2 high speed cutting steel substrates (steel disks, diameter is not higher than 30 mm, 5 mm thickness, in a delivery state) under different deposition regimes. A second series of substrates with 2 mm thickness and 20 mm diameter were used for RBS, SEM, EDS, TEM, nano– and microhardness tests. Substrate surface was treated using glow discharge in order to clean and activate it before deposition. For multilayer TiN/MoN coatings deposition we used a vacuum-arc device Bulat-6 with two evaporators (Ti and Mo) [10], which allows deposition of nanostructured coatings in pulsed mode with variable pulse amplitude and pulse frequency.

RBS technique was used to obtain full information about element composition of the coatings. Microstructure and element composition investigations were done using several scanning electron microscopes: Quanta 200 3D, Quanta 600 FE-SEM being equipped with PEGASUS 2000 X-ray detector, and a JEOL-7001F-TTLS with microanalysis Energy dispersive X-ray spectroscopy (EDS) unit. Depth profile analysis was done using 500 nA, 1.72 keV Ar+ primary ion beam at 450 incidence angle. SAJW-05 SIMS analyser was equipped by Physical Electronics 06-350E ion gun and QMA-410 Balzers quadrupole mass analyser with 16 mm diameter rods. Structure and phase composition was studied by X-ray Diffraction (XRD) using a Bruker Advanced D8 goniometer operating in Bragg-Brentano configuration with Cu-Kα radiation. Volume fraction of phases in the coating was calculated using standard method, taking into account integral intensity.

Samples were also investigated by cross-sectional transmission electron microscopy (XTEM) in high-resolution, bright-field, dark-field and selected area electron diffraction (SAED) modes using on a JEOL 2200-FS equipped with a field-emission gun and an omega energy filter. Chemical mapping was made on a JEOL-2100 LaB6 device equipped with a Jeol EDS system. Both TEMs were operated at 200 kV. Measurements of hardness and Young modulus were done using instrumented microhardness CSM REVETEST apparatus (Switzerland), tribological tests were done using tribometer, fabricated by CSM Instruments Company.

3. RESULTS AND DISCUSSION

The elemental composition of the samples was examined by RBS as well as EDS on cross-sectional images. RBS spectrum for TiN/MoN coatings with period 50 nm is presented on the Fig. 1a. We can see kinematic factors for Ti and Mo near the surface, but we can also see "modulations" and we are able to estimate the

---

thickness of individual layer from them. So, choosing amount of channels and knowing ion loss per one channel we can evaluate an average thickness of the layer on the cross-section of the analyzing beam. Thus, we can say, that the thickness of MoN layer equals to 16.2 nm. Using RBS spectrum data we can estimate the thickness of the first four layers from the surface, and we should point, that the thickness of TiN layer is around 33.8 nm, it is more than twice thicknesses of MoN layer. Results of SIMS analysis of the TiN/MoN coating with 50 nm period are presented in the insert of the Fig. 1a. Taking into account ion's energy loss, detector's resolution and the etching rate of Ar ions a value of 48.7 nm is obtained, in good agreement with RBS data and SEM observations.

The XRD patterns of the TiN/MoN multilayers with λ = 25, 50 and 100 nm are reported in Fig. 1b. Two main reflections are observed around 36.5 and 42.5°. The peak at 36.5° is attributed to (111)-oriented TiN grains. These results suggest that TiN/MoN multilayers consist of highly-textured (200) cubic layers, if one compares to the intensity ratio expected for bulk polycrystalline reference powders [11 – 13].

The volume fraction of TiN and γ-Mo_2N phases was extracted from the XRD line using the "New_profile" software (KhPI, Kharkiv, Ukraine). For 25 nm period, a TiN/ γ-Mo_2N ratio of 90/10 is obtained. Increasing of the period of TiN/MoN layers up to 50 nm led to forming of two-phases structure state with an average content of TiN and γ-Mo_2N cubic phases equal to 60 vol.%
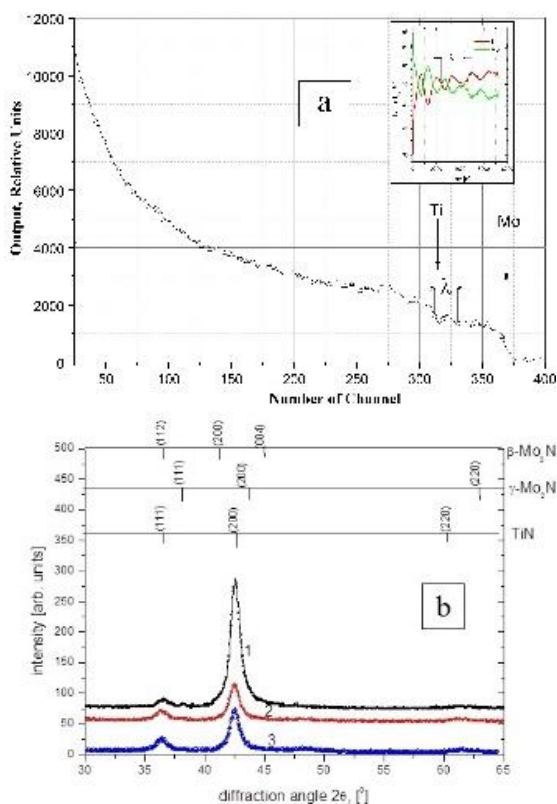

Fig. 1 – a – RBS spectrum of the 4 He+ ions backscattering for sample 2 in Table 1 with TiN/MoN coating (SIMS depth profile analysis of normalized secondary ion currents is shown on the insert: m/z= 48 (Ti+) and 98 (Mo+), logarithmic scale is to the left; b – XRD patterns for coatings with different bilayer periods (25 nm – curve 1, 50 nm – curve 2 and 100 nm – curve 3).

Table 1 – Parameters of coating's deposition

#	Material	Period, nm	I, A	Time, Sec, Ti/Mo	U_{bias}, V	U, V	Pulse Fr., kHz	Pressure, Pa
1		8	90	3/3			6	
2	TiN/ MoN	25	100	10/10	-40	1000	7	0. 5
3		50	100	20/20			7	
4		100	100	40/40			7	

and 40 vol.%. It correlates with Ti and Mo concentrations, obtained using EDX, equal to 62.3 at.% and 36.8 at.% accordingly. For samples with more thick TiN and Mo_2N layers (≈ 100 nm period) volume fraction of phases corresponds to EDX analysis data - 70 at.% for TiN and 30 at.% for Mo_2N.

It should be noted that in molybdenum nitride layers only the γ-Mo_2N with cubic, Na-Cl type lattice was formed while the ß-Mo_2N phase (tetragonal lattice) cannot be seen using XRD despite of the fact that both phases can be formed in the case of coating' deposition using vacuum-arc method and magnetron sputtering. It can be explained by two-stage process of forming of phase composition of the multilayered coating. In the early growth stage, a template effect occurs due to small lattice mismatch (< 2%) between cubic TiN (aTiN= 0.4242 nm, see JCPDS file n° 38-1420) and cubic Mo_2N (aMo2N= 0.4163 nm, see JCPDS file n° 25-1366) phases, promoting the stabilization of γ-Mo_2N cubic modification by atomic registry.

Cross-section SEM micrographs of the nanostructured coating is presented on the Fig. 2a, alternating nanoscale layers can be easily seen on the Fig. 2b, dark layers correspond to TiN, light layers correspond to MoN.
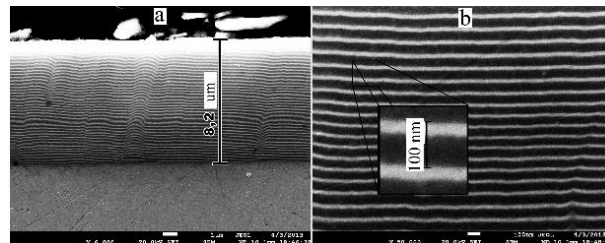

Fig. 2 – Cross-sectional SEM micrograph of TiN/MoN multilayer coating with 100 nm period: a – general view, thickness is 8.2 µм; b – higher magnification (x 50 000) showing individual layer thickness.

High resolution microscopy (HR-TEM) was used to characterize the structure of the multilayered system with the 50 nm average period. The TEM bright-field and dark-field images in Fig. 3 show columnar growth of the multilayer nitride system. It starts from interface between the {111} textured steel substrate and the multilayer, or from within the multilayer.
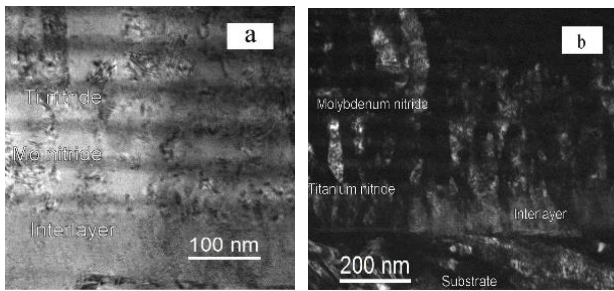
Fig. 3 – TEM bright field (a) and dark field (b) images showing the substrate, the interlayer and the TiN and MoN layers.

Slightly bent grains extend across nitride layers and interfaces, and are $20 \div 100$ nm large and $100 \div 500$ nm long. A 100 nm thin interlayer is visible and contains Ti, Mo, C and traces of N as evidenced by EDS mapping. This interlayer doesn't show any texture, is well crystallized and also contains columnar grains. A structural modulation with a period about 5 nm can be seen within the interlayer, as shown in the bright-field and Fast-Fourier-Transform (FFT) images in Fig. 4. This type of modulation has been observed in several metallic carbides which contain Ti or Mo and exhibit a superstructure due to the incorporation of impurity atoms in the lattice.

The first layer grown on top of this interlayer is a 5 nm thin titanium nitride, then followed by a 20 nm molybdenum nitride and a 40 nm titanium nitride again (see Fig. 3). The sequence was then repeated until the multilayer reached a total thickness of about 8 μm. It has been reported that (Mo, Ti)C compound is fcc with a lattice parameter a ~ 0.426 nm. The mismatch with TiN being close to zero, which allows for local epitaxy (111)MoTiC // (111)TiN.
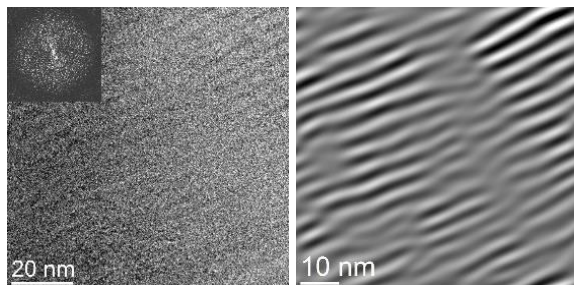

Fig. 4 – TEM bright-field (a) and FFT-filtered image (b) of the interlayer grown between the substrate and the multilayer. The FFT in shown in inset.

A typical diffraction pattern from the multilayer is shown in Fig. 5a. Here an area encompassing about 10 alternating layers was selected. Spots randomly distributed on circles labeled from 1 to 5 indicate layers with polycrystalline character. All spots in this diffraction pattern could be indexed with reflections belonging to fcc TiN and cubic γ-Mo_2N. Adjacent circles n°1 and 2 cross 111 spots and bear witness for local lattice parameter variation of about 2–3% within the nitride layers, so do circles 4 and 5 which cross 220 spots, while circle 3 goes through 200 spot. In the high-resolution TEM image shown in Fig. 5b, both titanium and molybdenum nitride layers appear well crystallized with thicknesses of 40 ± 5 nm and 20 ± 5 nm, respectively. Partial epitaxy occurs between adjacent

Mo_2N and TiN layers. Randomly oriented and distributed Moiré patterns extending over few nanometers are frequently observed, especially in molybdenum nitride layers. All layers are only weakly textured (if at all) with {100} orientation seen more frequently than {111}. Titanium nitride layers contain $5 \div 30$ nm size grains and are unambiguously identified as stoichiometric TiN. From most HRTEM images of the molybdenum nitride layers, all of which are fine grained ($5 \div 10$ nm size), a good match was found with γ-Mo_2N. However, in some cases FFTs reveal interplanar distances corresponding to non-cubic molybdenum nitrides – possibly strongly distorted Mo_2N or tetragonal Mo_2N – as reported by other authors [14]. FFTs acquired at few microns from the substrate in the molybdenum nitride layer, showed some SAED spots (such as one yielding an interplanar distance of 0.185 nm) that were consistent with 02-22 reflection from hexagonal MoN. The main reason for two-phase state appearing was intensive ion bombardment, which led to nanograins grinding and forming of interphase boundaries. Separate γ-Mo_2N layers with cubic lattice were formed and it caused forming of interphase boundary.

We investigated mechanical characteristics using nanoindentation method and we found, that the highest hardness of ~41.8 GPa was achieved for 8 nm period multilayered coating. Increasing of the period to 100 nm or decreasing to 25 nm led to decreasing of the hardness to the value of 26 GPa, which is rather similar to the value of hardness of single-layered TiN coating (about 23 GPa). Maximal value of the elasticity modulus E = 456 GPa corresponds to 25 nm period, and its value decreases with the increasing of the period.
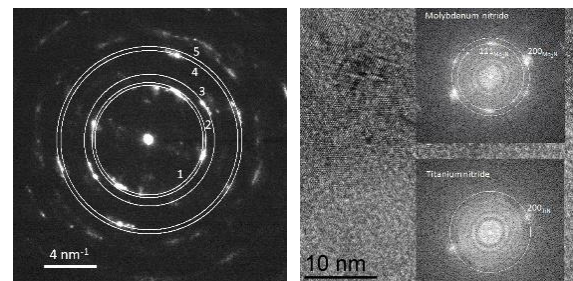

Fig. 5 – SAED pattern from the multilayer (a) and FFTs from the HRTEM images of the titanium and molybdenum nitride layers (b).

Thus, the obtained multilayered coatings have high hardness, which is more than 25% higher than the hardness of composing nitrides. Plasticity index is rather high and it allows using such coatings as protective under the influence of different alternating loadings and abrasive wear [15 – 17]. For multilayered TiN/MoN system we found, that the lowest value of Lc3 critical loading was 42.5 N, and it corresponds to periodical structure with the biggest period of 100 nm. If the period was 50 nm these critical loading value increased up to 61.0 N, and for the smallest 25 nm period Lc3 reached 64.8 N. Thus, using of very thin layers in multilayered system leads to increasing of specific density of interphase boundaries per volume units, in turn, it leads to increasing of critical loading of destruction.

4. CONCLUSION

Using C-PVD method we fabricated multilayered TiN/MoN coatings with different 8, 25, 50 and 100 nm layer's size. For such coatings we found, that maximal hardness and elasticity modulus were observed for 8 nm and 25 nm period accordingly. The lowest value of critical loading was 42.5 N, it corresponds to periodical structure with the biggest period of 100 nm. If the period was 50 nm the critical loading value increased up to 61.0 N, and for the smallest 8 nm period critical load reached 64.8 N. Thus, using of very thin layers in multilayered system leads to increasing of specific density of interphase boundaries per volume units and it leads to increasing of critical loading of destruction.

REFERENCES

1. Q. Meng, M. Wen, P. Liu, K. Zhang, W. Zheng, *Mater. Lett.* **94**, 61 (2013).
2. G. Abadias, Ph. Guerin, *Appl. Phys. Lett.* **93 (11)**, 111908, (2008).
3. H. Soderberg, M. Oden, T. Larsson, L. Hultman, Molina-J.M. Aldareguia, *Appl. Phys. Lett.* **88 (19)**, 191902 (2006).
4. A.D. Pogrebnjak, A.G. Ponomarev, A.P. Shpak, Yu.A. Kunitskii, *Phys. Usp.* **55 (3)**, 270 (2012).
5. A.D. Pogrebnjak, S.N. Bratushka, V.I. Boyko, I.V. Shamanin, Yu.V. Tsvintarnaya, *NIM B.* **145 (3)**, 373 (1998).
6. M. Nordin, M. Larsson, S. Hogmark, *Surf. and Coat. Tech.* **106**, 234 (1998).
7. J. Musil, *Surf. and Coat. Tech.* **207**, 50 (2012).
8. I.N. Martev, D.A. Dechev, N.P. Ivanov, Ts.D. Uzunov, E.P. Kashchieva, *J. Phys.: Conf. Series* **223 (1)**, 012 (2010).
9. A.D. Pogrebnjak, A.P. Shpak, N.A. Azarenkov, V.M. Beresnev, *Phys. Usp.* **52 (1)**, 29 (2009).
10. A.D. Pogrebnjak, V.M. Beresnev, *Nanocoatings, Nanosystems, Nanotechnologies.* (Bentham Sci. Publ.: 2012).
11. G. Abadias, V.I. Ivashchenko, L. Belliard, Ph. Djemia, *Acta Mater.* **60**, 5601 (2012).
12. U. Welzel, J. Ligot, P. Lamparter, A.C. Vermeulen, E.J. Mittemeijer, *J. Appl. Cryst.* **38**, 1 (2005).
13. J.-D. Kamminga, Th.H.de Keijser, R. Delhez, E.J. Mittemeijer, *J. Appl. Phys.* **88**, 6332 (2000).
14. D. Machon, D. Daisenberger, E. Soignard, E. Shen, T. Kawashima, E. Takayama-Muromachi, P.F. McMillan, *phys. status solidi a* **203 (5)**, 831 (2006).
15. A.D. Pogrebnjak, *J. of Nanomater.* ID 780125 (2013).
16. Guojun Zhang, Tianxiang Fan, Tao Wang, Hailin Chen, *Appl. Surf. Sci.* **274**, 231 (2013).
17. A.D. Pogrebnjak, V.M. Beresnev, O.V. Bondar, G. Abadias, P. Chartier, B.A. Postolnyi, A.A. Andreev, O.V. Sobol, *Tech. Phys. Lett.* **40 (3)**, 215 (2014).